Inorg. Chem. **2003**, *42*, 3873–3883

Do Penta- and Decaphospha Analogues of Lithocene Anion and Beryllocene Exist? Analysis of Stability, Structure, and Bonding by Hybrid Density Functional Study

E. J. Padma Malar*

Department of Physical Chemistry, University of Madras, Guindy Campus, Chennai 600 025, India

Received January 1, 2003

Stability in penta- and decaphospha analogues of lithocene anion and beryllocene is investigated by complete structural optimization at the B3LYP/6-31G* level. Natural bond orbital analysis is carried out to examine the bonding between the metal and the ligands. The heterolytic dissociation energies of 667 and 608 kcal/mol predicted by B3LYP/6-311+G**//B3LYP/6-31G* calculations for $CpBeP_5$ and $(P_5)_2Be$ are comparable with the observed value of 635 ± 15 kcal/mol in ferrocene. The high stability in $CpBeP_5$ and $(P_5)_2Be$ shows that these species are isolable under appropriate conditions. Lithocene anion and its phospha analogues possess lower stability toward dissociation into ionic fragments. A novel observation of the present study is that $CpBeP_5$ and $(P_5)_2Be$ have lowest energies when the two planar ligands are arranged perpendicular to each other such that one of the ligands, cyclo-P_5, is η^1-coordinated while the second ligand is η^5-coordinated to Be. The resulting structure having C_s point group (denoted as C_s(p)) is predicted to be 22 and 28 kcal/mol lower than the staggered sandwich geometry in $CpBeP_5$ and $(P_5)_2Be$, respectively, at the B3LYP/6-311+G**//B3LYP/6-31G* level. In the analogous lithocene anions $[CpLiP_5]^-$ and $[(P_5)_2Li]^-$ also the C_s(p) structures are found to be the lowest energy structures, though their relative stabilities are small. We also characterized the geometry with both ligands η^1-coordinated to the metal in a linear arrangement having the D_{2h} point group in the decaphospha analogues $[(P_5)_2Li]^-$ and $(P_5)_2Be$. This structure is found to be higher in energy than the C_s(p) structure. The D_{2h} structure could not be located as a potential minimum in the biscyclopentadienyl complexes and their pentaphospha analogues. Both the C_s(p) and D_{2h} structures are characterized for the first time in metallocenes. The D_{2h} structure seems to be a unique feature in the decaphospha metallocenes under consideration. Covalent bond formation between beryllium and phosphorus atom P_1 of η^1-(cyclo-P_5) is more pronounced (bond orders 0.43–0.49) than that between Be and C_1 of η^1-Cp (bond orders 0.24–0.27). Though both η^1-coordinated cyclo-P_5 and Cp exhibit C_{2v} point groups, bond alternation is less pronounced in the former. The Wiberg P–P bond orders in the η^1-(cyclo-P_5) of $CpBeP_5$ and $(P_5)_2Be$ having C_s(p) structures are in the range 1.29–1.47. These ring bond orders indicate that the P_5 ring retains aromaticity to a large extent in the η^1-mode of bonding with Be. Second-order perturbational energy analysis of the Fock matrix in the natural bond orbital basis reveals that there is a significant stabilizing interaction of ∼123 kcal/mol between the lone pair orbital of P_1 and the 2s orbital of Be in the C_s(p) structures.

Introduction

Cyclo-P_5, the pentaphospha analogue of the very common and versatile ligand cyclopentadienyl C_5H_5 (Cp), is receiving considerable attention in organometallic chemistry.[1−3] The first carbon-free entirely inorganic sandwich complex $[(\eta^5\text{-}P_5)_2Ti]^{2-}$ was synthesized and characterized by Urnezius et al.[4] Earlier attempts to prepare bis(cyclo-P_5) metallocenes led to high molecular weight solids.[5] A number of mixed

* Research Scientist, University Grants Commission, New Delhi, India. E-mail: ejpmalar@vsnl.net.

(1) Elschenbroich, C.; Salser, A. *Organometallics—A Concise Introduction*; VCH Verlagsgesellschaft: Weinheim, Germany, 1989.

(2) (a) Scherer, O. J. *Comments Inorg. Chem.* **1987**, *6*, 1. (b) Scherer, O. J. *Acc. Chem. Res.* **1999**, *32*, 751.

(3) Baudler, M.; Glinka, K. *Chem. Rev.* **1993**, *93*, 1623.

(4) Urnezius, E.; Brennessel, W. W.; Cramer, C. J.; Ellis, J. E.; Schleyer, P. v. R. *Science* **2002**, *295*, 832.

10.1021/ic0340027 CCC: $25.00
Published on Web 05/15/2003

sandwich metallocenes and triple-decker complexes containing cyclo-P_5 [(η^5-C_5Me_4R)M(η^5-P_5)] (M = Fe, Ru; R = Me, Et) and [(η^5-C_5Me_5)$_2$Cr(μ, η^5-P_5)] are well characterized.[2,6] Different theoretical studies have shown that cyclo-P_5^- is aromatic like the carbocyclic counterpart Cp^-.[7,8] Although in the sandwich complexes cyclo-P_5 is η^5-coordinated to the metal, other bonding modes such as η^1, η^3, μ-η^2: η^3, and μ-η^1 are not ruled out for the phosphorus heterocycle.[2b] Quantum chemical analysis of lone pair shapes in aza- and phosphaferrocenes led to the conclusion that η^5-coordination is characterized by both η^1- and η^2-interactions.[9] The lone pair at phosphorus can participate in η^1-coordination with the metal. Frunzke et al.[10] examined theoretically the ferrocene analogues (η^5-E_5)$_2$Fe (E = N, P, As, Sb) and showed that cyclo-P_5 leads to the strongest bonding in the series. The phosphorus complex (η^5-P_5)$_2$Fe is as stable as ferrocene having a homolytic bond dissociation energy of 128.3 kcal/mol which is close to that of ferrocene (131.3 kcal/mol). These findings are of immense interest as they illustrate the potential of the P_5 ring as a ligand and can lead to a wealth of interesting complexes parallel to their organic counterparts.[11] Metallocenes containing the phospholyl ligand are reported to be versatile catalysts especially in asymmetric synthesis.[12] Like their carbocyclic counterparts, the complexes containing poly-phosphorus ligands can also find application as building blocks for multidecker complexes and new materials.[11,13,14]

Metallocenes of the main group elements have been subjected to extensive research in recent years.[1,13−15] Different structural features are accompanied by a variety of bonding modes such as η^5, η^1, η^3, μ-η^2: η^3, and μ-η^1: η^5.[1,13,14] The solid-state structure of [Cp_2Li]$^-$ shows almost perfectly staggered Cp rings.[16] The observed structure indicates the presence of η^5-coordinated Cp rings which are not slipped.[16] But in the isoelectronic beryllocene several structures with varying degrees of coordination of Cp rings were proposed on the basis of different experimental[17] and theoretical[18] findings. In the staggered sandwich D_{5d} structure both Cp ligands are η^5-coordinated (pentahapto) to Be. In the "slip-sandwich" arrangements (Figure 1), one of the Cp ring is η^5-coordinated while the second ligand is η^1-coordinated. A precise low-temperature crystal structure claimed the "slip-sandwich" arrangement.[17e] Gas-phase structural studies provide indirect evidence for a slipped and tilted structure wherein the two Cp rings are not parallel.[17b,h] Ab initio calculations at the Hartree−Fock level using different basis sets were not conclusive.[18a−h] This situation led to the identification of beryllocene as one of the difficult structural/energetic problems in inorganic chemistry.[18i] The recent growth in the application of density functional theory[19] (DFT) to a variety of chemical problems led Mire et al. to reinvestigate the structural features of beryllocene using different density functionals.[18i] Their study with four different DFT functionals at the DFT/6-311G*//DFT/6-31G* level correctly predicts the slipped and tilted structure (tilted C_s geometry) as the ground state with energy 0.85−5.33 kcal/mol lower than the D_{5d} structure.[18i] Structural optimization at the MP2 level could not even locate the tilted C_s structure in the potential energy surface, and the MP2 theory was proved to be a failure in studying beryllocene.[18i]

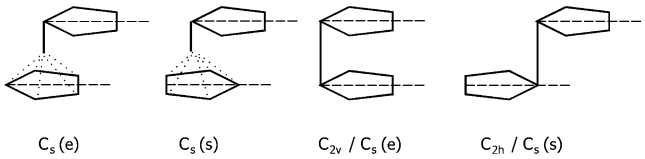

Figure 1. Slip-sandwich geometries subjected to structural optimization

Although the main group metallocenes have received considerable attention, studies on complexes containing P_5 rings are limited. Compounds of the type P_5M, M = Li, Na, and K, are prepared as stable solutions.[20] Electronic and

(5) Baudler, M.; Etzbach, *Angew. Chem., Int. Ed. Engl.* **1991**, *30*, 580.
(6) Scherer, O. J. *Angew. Chem., Int. Ed. Engl.* **1990**, *29*, 1104.
(7) Malar, E. J. P. J. *Org. Chem.* **1992**, *57*, 3694.
(8) Dransfeld, A.; Nyulaszi, L.; Schleyer, P. v. R. *Inorg. Chem.* **1998**, *37*, 4413.
(9) Frison, G.; Mathey, F.; Sevin, A. *J. Phys. Chem. A* **2002**, *106*, 5653.
(10) Frunzke, J.; Lein, M.; Frenking, G. *Organometallics* **2002**, *21*, 3351.
(11) Dillon, K. B.; Mathey, F.; Nixon, J. F. *Phosphorus: The Carbon Copy*; Wiley: Chichester, U.K., 1998.
(12) (a) Tanaka, K.; Fu, G. C. *J. Org. Chem.* **2001**, *66*, 8177. (b) Tanaka, K.; Qiao, S.; Tobisu, M.; Lo, M. M.-C.; Fu, G. C. *J. Am. Chem. Soc.* **2000**, *122*, 9870. (c) Qiao, S.; Flu, G. C. *J. Org. Chem.* **1998**, *63*, 4168.
(13) (a) Togni, A.; Halterman, L. *Metallocenes: Synthesis, Reactivity, Applications*; Wiley-VCH: Weinheim, Germany, 1998. (b) Long, N. J. *Metallocenes*; Blackwell Science: Oxford, U.K., 1998.
(14) (a) Jutzi, P.; Burford, N. *Chem. Rev.* **1999**, *99*, 969. (b) Green, J. C. *Chem. Soc. Rev.* **1998**, *27*, 263.
(15) (a) Hanusa, T. P. *Polyhedron*. 1**990**, *9*, 1345. (b) Hanusa, T. P. *Chem. Rev.* 1**993**, *93*, 1023. (c) Timofeeva, T. V.; Lii, J.-H.; Allinger, N. L. *J. Am. Chem. Soc.* **1995**, *117*, 7452. (d) Kaupp, M.; Schleyer, P. v. R.; Dolg, M.; Stoll, H. *J. Am. Chem. Soc.* **1992**, *114*, 8202. (e) Hanusa, T. P. *Organometallics* **2002**, *21*, 2559. (f) Smith, J. D.; Hanusa, T. P. *Organometallics* **2001**, *20*, 3056. (g) Morrison, C. A.; Wright, D. S.; Layfield, R. A. *J. Am. Chem. Soc.* **2002**, *124*, 6775.
(16) (a) Harder, S.; Prosenc, M. H. *Angew. Chem., Int. Ed. Engl.* **1994**, *33*, 1744. (b) Stalke, D. *Angew. Chem., Int. Ed. Engl.* **1994**, *33*, 2168. (c) Eiermann, M.; Hafner, K. *J. Am. Chem. Soc.* **1992**, *114*, 135. (d) Paquette, L. A.; Bauer, W.; Sivik, M. R.; Bhül, M.; Feigel, M.; Schleyer, P. v. R. *J. Am. Chem. Soc.* **1990**, *112*, 8776.
(17) (a) Almenningen, A.; Bastiansen, O.; Halland, A. *J. Chem. Phys.* **1964**, *40*, 3434. (b) Morgan, G. L.; McVicker, G. B. *J. Am. Chem. Soc.* **1968**, *90*, 2789. (c) McVicker, G. B.; Morgan, G. L. *Spectrochim. Acta* **1970**, *26A*, 23. (d) Almenningen, A.; Haaland, A.; Lusztyk, J. *J Organomet. Chem.* **1979**, *170*, 271. (e) Nugent, K. W.; Beattie, J. K.; Hambley, T. W.; Snow, M. R. *Aust. J. Chem.* **1984**, *37*, 1601. (f) Nugent, K. W.; Beattie, J. K. *J. Chem. Soc., Chem. Commun.* **1986**, 186. (g) Nugent, K. W.; Beattie, J. K. *Inorg. Chem.* **1988**, *27*, 4269. (h) Nugent, K. W.; Beattie, J. K.; Field, L. D. *J. Phys. Chem.* **1989**, *93*, 5371. (i) Nugent, K. W.; Beattie, J. K. *Inorg. Chim. Acta* **1992**, *198*, 309.
(18) (a) Haaland, A. *Acta Chem. Scand.* **1968**, *22*, 3030. (b) Chiu, N.-S.; Schäfer, L. *J. Am. Chem. Soc.* **1978**, *100*, 2604. (c) Marynick, D. S. *J. Am. Chem. Soc.* **1977**, *99*, 1436. (d) Jemmis, E. D.; Alexandratos, S.; Schleyer, P. v. R.; Streitwieser, A., Jr.; Schaefer, H. F., III. *J. Am. Chem. Soc.* **1978**, *100*, 5695. (e) Gleiter, R.; Böhm, M. C.; Haaland, A.; Johansen, R.; Lusztyk, J. *J Organomet. Chem.* **1979**, *170*, 285. (f) Margl, P.; Schwarz, K.; Blöchl, P. E. *J. Am. Chem. Soc.* **1994**, *116*, 11177. (g) Margl, P.; Schwarz, K.; Blöchl, P. E. *J. Chem. Phys.* **1995**, *103*, 683. (h) Schwarz, K.; Nusterer, E.; Margl, P.; Blöchl, P. E. *Int. J. Quantum Chem.* **1997**, *61*, 369. (i) Mire, L. W.; Wheeler, S. D.; Wegenseller, E.; Marynick, D. S. *Inorg. Chem.* **1998**, *37*, 3099.
(19) (a) Hohenberg, P.; Kohn, W. *Phys. Rev. B* **1964**, *136*, 864. (b) Parr, R. G.: Yang, W. *Density Functional Theory of Atoms and Molecules*; Oxford University: New York, 1989.
(20) (a) Baudler, M.; Düster, D.; Ouzounis, D. *Z. Anorg. Allg. Chem.* **1987**, *544*, 87. (b) Baudler, M.; Ouzounis, D. *Z. Naturforsch.* **1989**, *44b*, 381. (c) Baudler, M.; Etzbach, Th. *Chem. Ber.* **1991**, *124*, 1159. (d) Baudler, M.; Akpapoglou, S.; Ouzounis, D.; Wasgestian, F.; Meinigke, B.; Budzikiewicz, H.; Münster, H. *Angew. Chem., Int. Ed. Engl.* **1988**, *27*, 280.

molecular structures of lithium and sodium derivatives of cyclo-P_5 have been studied by Hamilton and Schaefer[21a] and Schleyer and co-workers.[21b] There is no report so far on the bis(cyclo-P_5)metal complexes of the main group elements. The aim of the present study is to examine theoretically the nature of bonding, stability, and structures in the hitherto unknown penta- and decaphospha analogues of the simplest metallocenes, lithocene anion [Cp_2Li]$^-$ and beryllocene Cp_2-Be. The relative stabilities of these compounds are compared with those of the well-characterized parent metallocenes containing Cp^-.

Computational Aspects

All computations were performed with the Gaussian 94 program.[22] Structures of the complexes are examined by energy minimization with the 6-31G* basis set at the Hartree−Fock (HF), Møller−Plesset second-order perturbation theory (MP2), and density functional theory (DFT) levels. The present study invokes hybrid HF−DFT calculations with the three-parameter gradient-corrected exchange potential of Becke and the gradient-corrected correlation potential of Lee, Yang, and Parr (B3LYP).[23] A number of recent studies reveal that the DFT calculations yield dependable geometries and electronic properties in organometallic compounds.[4,18i,24] In order to examine the role of diffuse functions in the energetics and bonding in the systems under consideration that include anions/anionic components, single-point B3LYP/6-31+G* and B3LYP/6-311+G** calculations were done at B3LYP/6-31G* optimized geometries. We also performed single-point calculations using the triple split valence basis set without diffuse functions (B3LYP/6-311G*).

Electronic structure studies on the metallocenes of transition metals invoke effective core potentials (ECPs) on the heavier elements. In the present study we have also examined the suitability of B3LYP calculations involving ECPs on phosphorus atoms. The 10 core electrons of P are replaced by ECPs using the double-ζ valence basis set of Hay and Wadt[25] denoted as LANL2DZ. In this basis set Dunning and Hay's full double-ζ basis (D95) is used for the first-row atoms.[26]

Complete structural optimization is carried out on the eclipsed sandwich (D_{5h}/C_{5v}), the staggered sandwich (D_{5d}/C_{5v}), and the slipped (C_s) geometries of the complexes. Slip-sandwich geometries, where one of the ligands (cyclopentadienyl or cyclo-P_5) has η^1-coordination, are generated by moving the ligand away from the symmetric sandwich arrangement such that a ring atom (C_1 or P_1) becomes collinear with the metal center as well as the center of the second ligand, maintaining the ring planes parallel to each other (Figure 1). Slipping is done starting from both the eclipsed and the staggered sandwich arrangements. The slip-sandwich geometries possess C_s point group, and in the present study, we denote the structures as C_s(s) or C_s(e) to indicate slipping from staggered sandwich or eclipsed sandwich arrangement. In pentaphospha metallocene, there are four slipped sandwich arrangements allowing η^1-coordination to either Cp or P_5 ring. In addition to the slipped geometries in which one of the ligands has η^1-coordination, we also examined the structures in which both ligands are η^1-coordinated to the metal (Figure 1).

The bonding in the complexes is examined by natural bond orbital (NBO) analysis formulated in terms of natural atomic orbitals using the NBO program.[27] Ab initio wave functions transformed into NBOs are found to describe well the covalency effects in molecules.[28a,b] The advantage of natural population analysis (NPA) in predicting reliable estimates of charges on atomic centers is established in earlier studies.[28] Covalent bonding between the metal and the ligand atoms is studied using bond orders obtained from the natural bond orbitals by Wiberg's method.[29]

Results and Discussion

Table 1 presents the binding energy, ΔE, of the complexes with respect to heterolytic dissociation into metal cation and the anionic ligands in the different geometries. For a given complex LML′, ΔE is calculated using the equation

$$\Delta E = E(\mathrm{LML'}) - E(\mathrm{L}^-) - E(\mathrm{L'}^-) - E(\mathrm{M}^{n+})$$

In lithocene anions $n = 1$, and in beryllocenes $n = 2$. The total energies of the complexes and their ionic components are shown in the Supporting Information (Table S1). The negative of ΔE corresponds to the experimental heterolytic dissociation energy in the metallocene. The relative stabilities of the different structures in a given complex with reference to the staggered sandwich geometry are shown inside parentheses in Table 1. It is seen that the relative energies predicted by the HF/6-31G*, B3LYP/6-31G*, and B3LYP/LANL2DZ methods reflect a uniform trend in general, but the MP2/6-31G* calculations predict trends that are often different from the remaining methods. Marynick[18i] and co-workers have demonstrated that MP2/6-31G* is a failure in studying beryllocene. In our study on decaphosphaberyllocene, we faced difficulty in characterizing the D_{5h} structure at MP2/6-31G* level. Attempts to optimize the D_{5h} geometry yielded a high-energy structure, 14.8 kcal/mol higher than the D_{5d} arrangement. The resulting D_{5h} structure is found to have the unduly short separation of 1.272 Å between Be and the center of the P_5 ring as against a value of 1.752 Å in the D_{5d} geometry. Thus the present analysis also proves that the MP2/6-31G* calculations are unsuitable to examine the cyclo-P_5 analogues of beryllocene. The DFT methods, on

(21) (a) Hamilton, T. P.; Schaefer, H. F., III. *Angew. Chem., Int. Ed. Engl.* **1989**, *28*, 485. (b) Glukhovtsev, M. N.; Schleyer, P. v. R.; Maerker, C. *J. Phys. Chem.* **1993**, *97*, 8200.
(22) Frisch, M. J.; Trucks, G. W.; Schlegel, H. B.; Gill, P. M. W.; Johnson, B. G.; Robb, M. A.; Cheeseman, J. R.; Keith, T.; Petersson, G. A.; Montgomery, J. A.; Raghavachari, K.; Al-Laham, M. A.; Zakrzewski, V. G.; Ortiz, J. V.; Foresman, J. B.; Peng, C. Y.; Ayala, P. Y.; Chen, W.; Wong, M. W.; Andres, J. L.; Replogle, E. S.; Gomperts, R.; Martin, R.; Fox, D. J.; Binkley, J. S.; Defrees, D. J.; Baker, J.; Stewart, J. P.; Head-Gordon, M.; Gonzalez, C.; Pople, J. A. *Gaussian 94*, revision B.2; Gaussian, Inc.: Pittsburgh, PA, 1995.
(23) (a) Becke, A. D. *J. Chem. Phys*. **1993**, *98*, 5648. (b) Lee, C.; Yang, W.; Parr, R. G. *Phys. Rev. B* **1988**, *37*, 785.
(24) See for instance: (a) References cited in ref 18i. (b) Kenny, J. P.; King, R. B.; Schaefer, H. F., III. *Inorg. Chem*. **2001**, *40*, 901. (c) Maron, L.; Eisenstein, O. *J. Phys. Chem. A* **2000**, *104*, 7140. (d) Matsuzawa, N.; Seto, J.; Dixon, D. A. *J. Phys. Chem. A* **1997**, *101*, 9391.
(25) Hay, P. J.; Wadt, W. R. *J. Chem. Phys*. **1985**, *82*, 270, 284, 299.
(26) Dunning, T. H., Jr.; Hay, P. J. In *Modern Theoretical Chemistry*; Schaefer, H. F., III, Ed.; Plenum Press: New York, 1976; pp 1−28.
(27) (a) Foster, J. P.; Weinhold, F. *J. Am. Chem. Soc*. **1980**, *102*, 7211. (b) Glendening, E. D.; Reed, A. E.; Carpenter, J. E.; Weinhold, F. *NBO Version 3.1*; University of Wisconsin, Wisconsin, 1990.
(28) (a) Reed, A. E.; Weinstock, R. B.; Weinhold, F. *J. Chem. Phys*. **1985**, *83*, 735. (b) Reed, A. E.; Curtiss, L. A.; Weinhold, F. *Chem. Rev*. **1988**, *88*, 899. (c) Lambert, C.; Schleyer, P. v. R. *Angew. Chem., Int. Ed. Engl*. **1994**, *33*, 1129.
(29) Wiberg, K. B. *Tetrahedron* **1968**, *24*, 1083.

Table 1. Stabilization Energies ΔE and the Relative Energies (inside Parentheses) at Optimized Geometries

		ΔE (kcal/mol)			
system	point group	HF/6-31G*	MP2/6-31G*	B3LYP/6-31G*	B3LYP/LANL2DZ
$[Cp_2Li]^-$	D_{5h}	−231.00 (0.00)	−246.64 (−0.04)	−236.92 (0.05)	−221.40 (0.01)
	D_{5d}	−231.00 (0.00)	−246.60 (0.00)	−236.97 (0.00)	−221.41 (0.00)
$[CpLiP_5]^-$	C_{5v}(e)	−198.99 (0.02	−220.40 (−0.10)	−205.48 (0.02)	−193.45 (0.00)
	C_{5v}(s)	−199.01 (0.00)	−220.30 (0.00)	−205.50 (0.00)	−193.45 (0.00)
	C_s(p)	−204.36 (−5.35)	−214.81 (5.49)	−209.72 (−4.22)	−199.29 (−5.84)
$[(P_5)_2Li]^-$	D_{5h}	−152.06 (0.12)	−185.87 (−0.17)	−161.14 (0.09)	−150.74 (0.11)
	D_{5d}	−152.18 (0.00)	−185.70 (0.00)	−161.23 (0.00)	−150.85 (0.00)
	C_s(p)	−156.00 (−3.82)	−176.59 (9.11)	−163.54 (−2.31)	−156.27 (−5.42)
	D_{2h}	−152.70 (−0.52)	−161.87 (23.83)	−158.24 (2.99)	−156.76 (−5.91)
Cp_2Be	D_{5h}	−718.33 (0.09)	−751.05 (0.12)	−733.99 (0.15)	−703.26 (0.20)
	D_{5d}	−718.42 (0.00)	−751.17 (0.00)	−734.14 (0.00)	−703.46 (0.00)
	C_s(e)	−724.82 (−6.40)		−736.76 (−2.62)	−710.35 (−6.89)
	C_s(s)	−724.76 (−6.34)		−736.70 (−2.56)	−710.40 (−6.94)
$CpBeP_5$	C_{5v}(e)	−644.47 (0.08)	−690.68 (0.53)	−665.89 (0.19)	−633.92 (0.05)
	C_{5v}(s)	−644.55 (0.00)	−691.21 (0.00)	−666.08 (0.00)	−633.97 (0.00)
	C_s(e)	−639.00 (5.55)	−687.25 (3.96)	−663.25 (2.83)	−630.16 (3.81)
	C_s(s)	−638.68 (5.87)	−684.58 (6.63)	−661.45 (4.63)	−628.66 (5.31)
	C_s(p)	−675.44 (−30.89)	−700.47 (−9.26)	−690.13 (−24.05)	−663.71 (−29.74)
$(P_5)_2Be$	D_{5h}	−546.57 (0.03)		−579.89 (0.18)	−542.71 (0.66)
	D_{5d}	−546.60 (0.00)	−614.53 (0.00)	−580.07 (0.00)	−543.37 (0.00)
	C_s(p)	−585.39 (−38.79)	−636.06 (−21.53)	−611.94 (−31.87)	−577.89 (−34.52)
	D_{2h}	−569.82 (−23.22)	−591.15 (23.38)	−591.82 (−11.75)	−577.69 (−34.32)

the other hand, are shown to be reliable, and hence we have focused on the B3LYP/6-31G* results in the discussion on structure and bonding characteristics of the systems under study. We performed frequency calculations at the B3LYP/6-31G* optimized lowest energy structure and the staggered sandwich structure. The lowest vibrational frequencies (including lowest real frequency) in these structures are included in the Supporting Information (Table S1). It is observed from the frequency calculations that the staggered sandwich geometries of $[CpLiP_5]^-$ and $CpBeP_5$ are characterized by two imaginary vibrational frequencies. The D_{5d} structure of decaphosphaberyllocene shows four imaginary frequencies each ∼100 i cm^{-1}. The frequency analysis thus reveals that the staggered sandwich geometries of $[CpLiP_5]^-$, $CpBeP_5$, and $(P_5)_2Be$ are higher order saddle points. The lowest energy C_s(p) structures of these metallocenes also show each one imaginary vibrational frequency having a value less than 20 i cm^{-1}. The low frequencies observed (excluding the translational and rotational modes) indicate the possibility of free rotation in the systems, as experimentally observed.[16a]

Energetics. The results presented in Table 1 reveal that the stabilization energies in the beryllocenes are considerably larger than that in the analogous lithocene anions at the different levels of calculation. For example, B3LYP/6-31G* predicts a stability of −734.14 kcal/mol with reference to heterolytic dissociation in the D_{5d} structure of beryllocene while it is −236.97 kcal/mol in lithocene anion. A comparison of the binding energies of metallocenes containing Cp and the cyclo-P_5 ligands reveals that the stability follows the order Cp_2M > $CpMP_5$ > $(P_5)_2M$. In beryllocene, substitution of one Cp ligand by a P_5 ring lowers the stability by ∼50 kcal/mol while the introduction of the second P_5 ligand lowers further the stability by ∼80 kcal/mol. In lithocene anion the corresponding values are 30 and 40 kcal/mol, respectively. Lowering of stability in the Cp anion by in-ring substitution of phosphorus atoms was noticed earlier.[7]

It is seen from Table 1 that the energy difference between the eclipsed sandwich and staggered sandwich geometries is negligibly small in all the species studied. The B3LYP/6-31G* calculations predict uniformly the staggered sandwich structure to be marginally lower in energy than the eclipsed sandwich structure. This is in agreement with the observation of staggered geometry for lithocene anion.[16] High anisotropy in the ring thermal parameters of lithocene anion is attributed to a small energy difference between the staggered and eclipsed conformations.[16a,b] It may also be noted that studies on metallocenes of transition metals and lanthanides also reveal a very small energy difference between staggered and eclipsed sandwich geometries.[9,24d,31] The slipped geometry could not be characterized as a potential minimum in lithocene anion.

In beryllocene, the slipped and tilted geometry is more favored than the symmetric sandwich arrangements (Figure 2). The optimized slipped geometries C_s(e) and C_s(s) of $BeCp_2$ are about 2.6 kcal/mol lower in energy than the staggered sandwich geometry at the B3LYP/6-31G* level. The relative stability of the slipped and tilted $BeCp_2$ predicted by both HF/6-31G* and B3LYP/LANL2DZ is slightly more than that of the B3LYP/6-31G* calculation. Although the prediction of the slipped and tilted structure as the ground state for beryllocene is in agreement with the experimental[17b,h] and earlier theoretical[18i] works, it is surprising that calculations on $CpBeP_5$ at various levels of the theory predict that the Cp-slipped structures C_s(e) and C_s(s) (Figure 3) are about 3−7 kcal/mol higher than the symmetric sandwich geometries.

B3LYP/6-31G* calculations predict that in penta- and decaphosphaberyllocenes the C_s(p) structure, in which the

(30) (a) Mayor-Lopez, M. J.; Weber, J. *Chem. Phys. Lett*. **1997**, *281*, 226. (b) Ryan, M. F.; Eyler, J. R.; Richardson, D. E. *J. Am. Chem. Soc.* **1992**, *114*, 8611.
(31) Orendt, A. M.; Facelli, J. C.; Jiang, Y. J. J.; Grant, D. M. *J. Phys. Chem. A* **1998**, *102*, 7692.

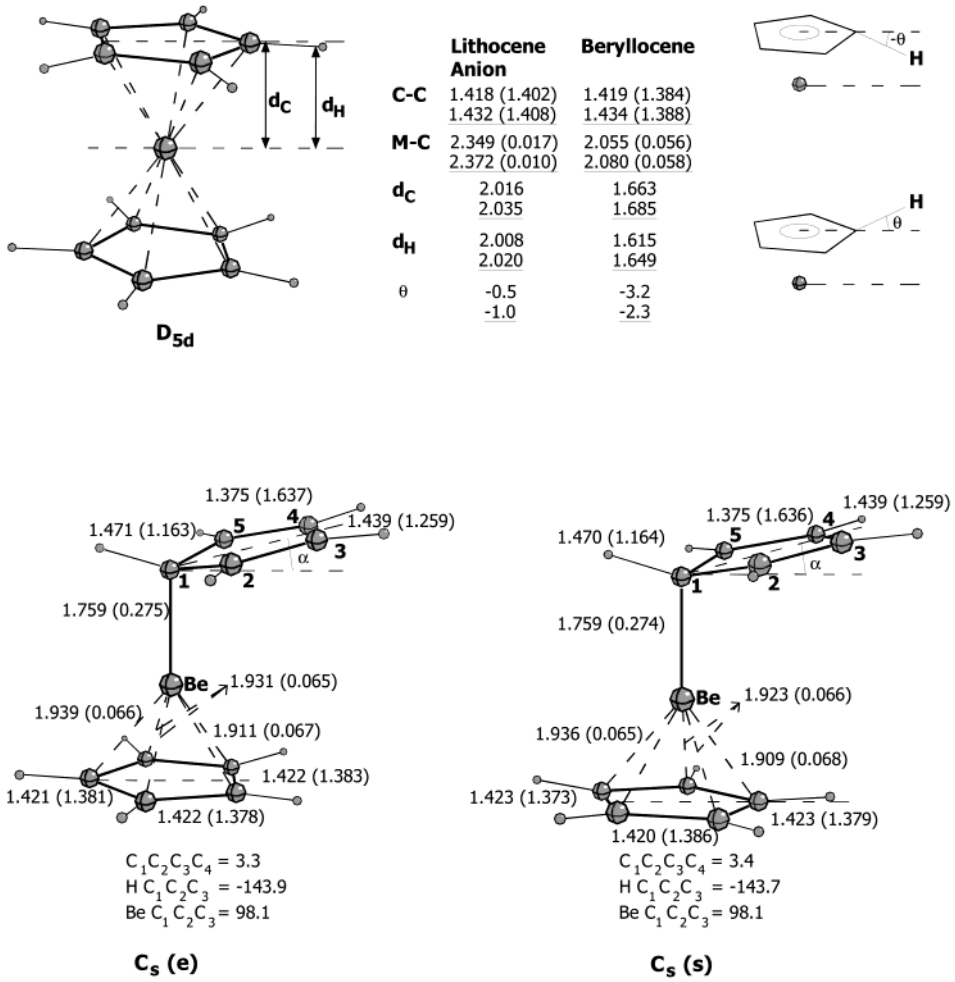

Figure 2. Optimized staggered sandwich geometries D_{5d} of lithocene anion and beryllocene and slipped geometries C_s(e) and C_s(s) of beryllocene. Bond lengths are given in angstroms and angles in degrees. Wiberg bond orders are given inside parentheses. The underlined values are B3LYP/LANL2DZ results.

η^1-coordinated P_5 plane is perpendicular to the η^5-coordinated Cp or P_5 plane, possesses the lowest energy. This structure is characterized for the first time in metallocenes. The C_s(p) structure is significantly lower in energy than the staggered sandwich geometry by 24.05 and 31.87 kcal/mol in $CpBeP_5$ and P_5BeP_5, respectively. Similar trends are also observed in the HF/6-31G*, MP2/6-31G*, and B3LYP/LANL2DZ calculations. In the isoelectronic penta- and decaphosphalithocene anions also B3LYP/6-31G* calculations predict the C_s(p) structure to be the lowest energy arrangement. However, the stabilization relative to the staggered sandwich structure is small and amounts to 4.22 and 2.31 kcal/mol in [CpLi P_5]$^-$ and [$(P_5)_2$Li]$^-$, respectively.

In the decaphospha analogues [$(P_5)_2$Li]$^-$ and $(P_5)_2$Be, the D_{2h} geometry of the metallocenes, in which both of the ligands are η^1-coordinated to the metal in a linear structure, is higher in energy than the C_s(p) arrangement. In $(P_5)_2$Be, the D_{2h} point group is lower than the D_{5h} and D_{5d} structures.

The stabilization energies obtained by incorporating diffuse function in the basis set at optimized B3LYP/6-31G* geometries are shown in Table 2. Both B3LYP/6-31+G* and B3LYP/6-311+G** calculations yield very similar binding energies. Although these calculations predict the same trend in the relative stabilities of the complexes under consideration, the inclusion of diffuse functions in the basis set lowers significantly the magnitude of binding energy in the metallocenes containing Cp ligand as compared to the value predicted by the polarized 6-31G* basis set. Thus in [Cp_2Li]$^-$ and Cp_2Be the stabilities are lowered by about 27 and 35 kcal/mol, respectively, according to B3LYP/6-311+G**//B3LYP/6-31G* calculations. In the corresponding pentaphospha analogues the stabilities are lowered by 13 and 23 kcal/mol. In the decaphospha analogues the decrease in stability observed with the 6-311+G** basis set is <4 kcal/mol. The B3LYP/6-311+G**//B3LYP/6-31G* values for the heterolytic dissociation energies are 667 and 608 kcal/mol respectively in the lowest energy structures of $CpBeP_5$ and $(P_5)_2$Be. These quantities are comparable to that of ferrocene, which is predicted by DFT to be 646−663 kcal/mol lower than two Cp^- and the ^{5}D state of Fe^{2+}.[10,30a] The experimental energy for heterolytic bond cleavage in Cp_2Fe is 635 ± 15 kcal/mol.[30b] The B3LYP/6-311+G**//B3LYP/6-31G* heterolytic dissociation energies of 667 and 608 kcal/mol in $CpBeP_5$ and $(P_5)_2$Be indicate that these species are nearly as stable as ferrocene and can be isolated under appropriate conditions.

Structure and Bonding in Lithocene Anion and Beryllocene. It is observed that the structural parameters of the

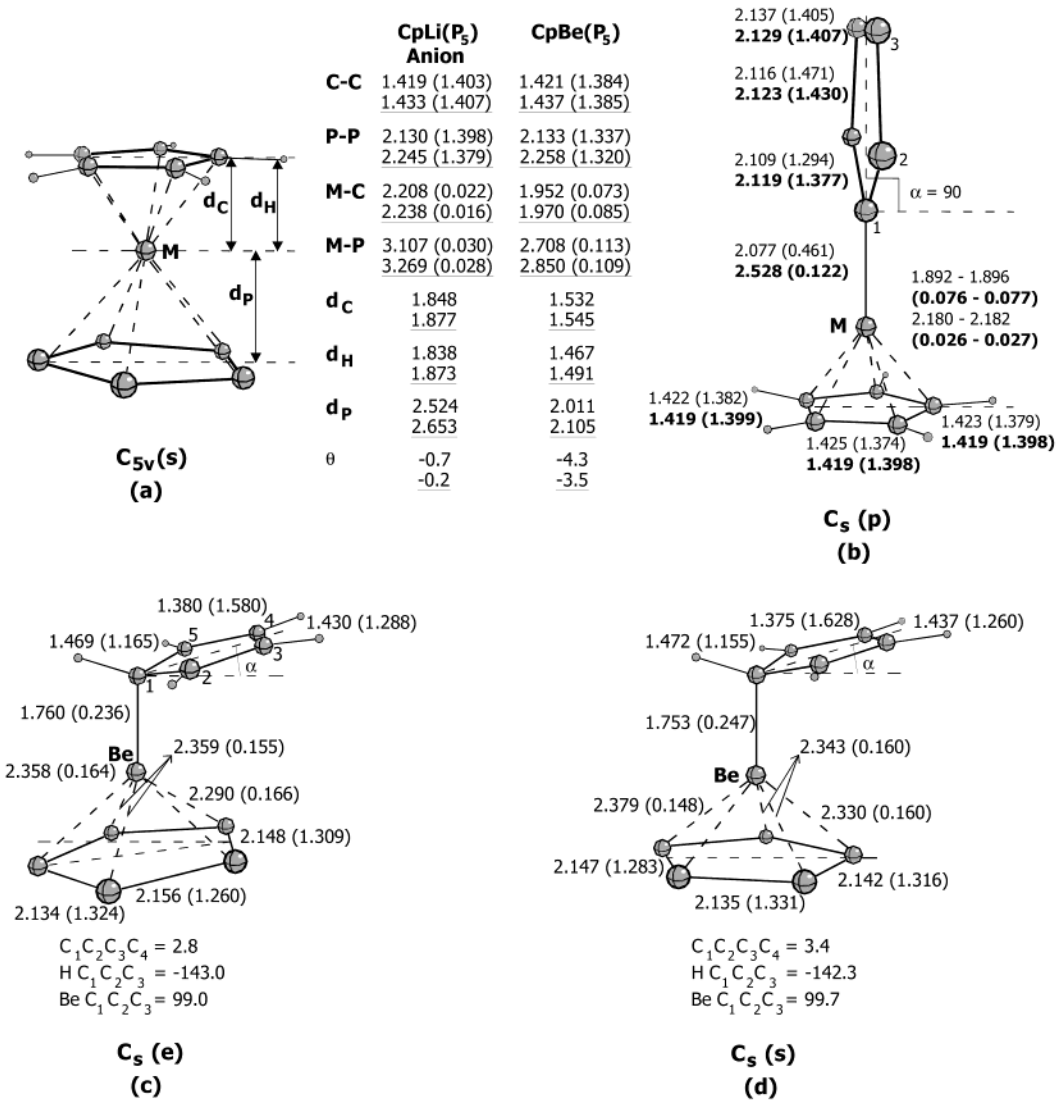

Figure 3. Optimized (a) staggered sandwich C_{5v} and (b) P_5-slipped C_s(p) geometries in $[CpLiP_5]^-$ and $CpBeP_5$; (c,d) Cp-slipped geometries of beryllocene. In part b the structural parameters of the lithocene anion analogue are shown in bold. Bond lengths are given in angstroms and angles in degrees. Wiberg bond orders are given inside parentheses. The underlined values are B3LYP/LANL2DZ results.

Table 2. Binding Energies (kcal/mol) in Lithocene Anion and Beryllocene and Their Phospha Analogues Using Basis Sets with Diffuse Functions, 6-31+G* and 6-311+G**[a]

system	point group	binding energy[b] B3LYP/6-311G*	B3LYP/6-31+G*	B3LYP/6-311+G**
$[Cp_2Li]^-$	D_{5d}	−223.16 (0.0)	−209.49 (0.0)	−209.70 (0.0)
$[CpLiP_5]^-$	C_{5v}(s)	−196.79 (0.0)	−186.94 (0.0)	−191.57 (0.0)
	C_s(p)	−201.14 (−4.35)	−191.63 (−4.69)	−196.42 (−4.85)
$[(P_5)_2Li]^-$	D_{5d}	−159.07 (0.0)	−154.86 (0.0)	−158.47 (0.0)
	C_s(p)	−161.62 (−2.55)	−157.73 (−2.87)	−161.94 (−3.47)
Cp_2Be	D_{5d}	−715.10 (0.0)	−699.72 (0.0)	−697.08 (0.0)
	C_s(e)	−719.36 (−4.26)	−703.78 (−4.06)	−701.84 (−4.76)
$CpBeP_5$	C_{5v}(s)	−653.88 (0.0)	−644.70 (0.0)	−645.76 (0.0)
	C_s(p)	−675.76 (−21.88)	−668.69 (−23.99)	−667.48 (−21.72)
$(P_5)_2Be$	D_{5d}	−578.82 (0.0)	−571.94 (0.0)	−580.00 (0.0)
	C_s(p)	−606.32 (−27.50)	−604.32 (−32.40)	−608.18 (−28.18)

[a] The relative energy with reference to the staggered sandwich structure is given inside parentheses. [b] At B3LYP/6-31G* optimized geometries.

ligands and the metal−ligand separation are nearly identical in both the staggered sandwich and the eclipsed sandwich geometries in Cp_2Li anion and Cp_2Be and also in their penta- and decaphospha analogues. Figure 2 depicts the B3LYP/6-31G* optimized D_{5d} geometries of Cp_2Li anion and Cp_2Be and the slipped geometries of Cp_2Be. Lithocene anion converged into the symmetric sandwich geometries even when optimization was initiated from the slipped sandwich arrangements.

The B3LYP/6-31G* value of 2.016 Å for the distance between Li and the plane containing the carbon atoms of the Cp ring, d_C (Figure 2), is in close agreement with the experimental value of 2.008 Å.[16a] In beryllocene d_C is shortened by about 0.5 Å, consistent with the smaller ionic radius of beryllium ($Be^{2+} = 0.31$ Å and $Li^+ = 0.60$ Å). Bond orders shown inside parentheses in Figure 2 reveal that there is negligible covalent bonding between the metal center and carbon atoms in the D_{5d} structure.

When slip-sandwich geometries C_s(e) and C_s(s) of beryllocene (Figure 1) are subjected to complete structural optimization, it is found that the η^1-coordinated Cp ligand is tilted away from the sandwich arrangement by an angle α (Figure 2). Further it is seen that the η^1-coordinated ligand is nonplanar in beryllocene with the unique carbon C_1 deviating by about 3° from the plane containing the remain-

ing carbon atoms. The hydrogen bonded to C_1 also deviates from the ring plane, resulting in the dihedral angle $HC_1C_2C_3 = -143.9°$. The dihedral angle $BeC_1C_2C_3$ is about 98° in the tilted structures C_s(e) and C_s(s) of beryllocene. In the slip-sandwich arrangement this angle is 90°. Consequently, the tilt angle α is estimated to be about 8° in $BeCp_2$.

The σ-bond length between Be and the unique carbon in the slipped structures of beryllocene is found to be 1.759 Å with a covalent bond order of about 0.27. The Be−C_1 bond order reflects that it is not like a normal single bond (having a bond order of about 1.0) and indicates that the bonding between Be and C_1 is not entirely covalent. Due to change in the nature of bonding around the carbon atom C_1 of the η^1-coordinated Cp, the ring exhibits C_{2v} symmetry, leading to notable bond alternation. The C−C bonds adjacent to C_1 are elongated to 1.471 Å, resulting in weakened aromatic bonds C_1-C_2 and C_1-C_5 with bond order 1.16. Though in the η^1-coordinated Cp π-electron ring current formation and, thus, the aromatic stabilization are reduced, hyperconjugative interaction involving the C_1−Be σ bond can introduce considerable stability as demonstrated by Nyulaszi and Schleyer[32] in cyclopentadiene disubstituted with electropositive groups. The NBO analysis reveals that the occupancy of the C_1−Be σ bond is 1.72 electrons and the electrons are polarized toward C_1 by 89.3%. The structural parameters in the η^5-coordinated Cp remain closer to the values in the D_{5d} arrangement. It is noticed that similar results are predicted by the B3LYP/LANL2DZ calculations also.

Positions of the hydrogen atoms in the lithocene anion could not be located in the crystal structure.[16a] The present study reveals that there is hardly any bending of hydrogen atoms away from the plane containing the carbon atoms. The bent angle of −0.5° (Figure 2) reveals that the hydrogens are bent away from the carbon plane toward the lithium center by 0.5°. Consequently the distance between Li and the plane containing the hydrogen atoms, $d_{H,}$ is lowered slightly to 2.008 Å. In (cyclopentadienyl)lithium, theoretical calculations predict that the bend angle decreases with increasing basis set.[33a] However, the out-of-plane bending of hydrogens toward Be is more pronounced in beryllocene with the bent angle $\theta = -3.2°$. This results in a lower value for d_H (1.615 Å) than d_C (1.663 Å). Many experimental and theoretical observations report on the bending of hydrogen atoms of the Cp ring, toward or away from the central metal atom, in metallocenes of main group elements and transition metals.[18d,33] Jemmis and Schleyer[18d] have explained hydrogen bending in terms of orbital overlap involving p-orbitals of the metal with those of the carbon atoms in Cp. Accordingly the direction of bending depends on the relative size of the metal p-orbitals. Metals with more diffuse p-orbitals favor hydrogens to bend away from the metal.[18d] The present more rigorous calculations reveal that hydrogens bend toward the metal in both metallocenes although it is very small in lithocene anion.

Structure and Bonding in Pentaphospha Analogues of Lithocene Anion and Beryllocene. The B3LYP/6-31G* optimized geometries of the pentaphospha analogues are shown in Figure 3. Structural optimization performed on Cp-slipped arrangements (both eclipsed and staggered) of pentaphosphalithocene anion led to the symmetric sandwich C_{5v} geometries. However, in the case of Cp-slipped sandwich geometries of $CpBeP_5$, structural optimization resulted in tilted geometries C_s(e) and C_s(s) wherein the plane of the slipped ring is no longer parallel to the cyclo-P_5 ligand (Figure 3). The structural and bonding parameters of the η^1-coordinated Cp are found to be very similar to those in the slipped structures of beryllocenes (Figure 2). The η^5-coordinated cyclo-P_5 unit shows significant deviation from D_{5h} symmetry. The Be−P distances are in the range 2.29−2.38 Å and are significantly shorter than the value of 2.708 Å in the C_{5v} geometry. The Be−P bond orders are increased by about 0.05 as compared to that of 0.11 in the sandwich structure.

Interestingly when the P_5 ring is slipped from the eclipsed as well as the staggered sandwich C_{5v} arrangements of $CpBeP_5$ and subjected to optimization, the P_5 plane becomes perpendicular to the Cp plane, resulting in the structure C_s-(p) with tilt angle $\alpha = 90°$and dihedral angle $BeP_1P_2P_3 = 180°$ (Figure 3). This observation is novel in that the C_s(p) structure is the lowest energy structure for pentaphosphaberyllocene. In this structural arrangement, the two planar ligands of the metallocence are perpendicular to each other and such geometry is predicted for the first time in metallocenes. In this structure, the atoms of the P_5 ring other than P_1 have negligible interactions with the central atom and the Cp ligand as the atoms are well separated. The Be−P_1 bond length and the bond order in the C_s(p) structure of $CpBeP_5$ are predicted to be 2.077 Å and 0.46, respectively. As compared to the bond order of ∼0.24 for the Be−C_1 bond in the C_s(e) and C_s(s) structures of $CpBeP_5$, it is clear that the extent of covalent bond formation between Be and P_1 is more pronounced in the C_s(p) structure. Similar to the η^1-Cp in beryllocene and $CpBeP_5$, the η^1-(cyclo-P_5) unit in $CpBeP_5$ also exhibits C_{2v} symmetry. The P−P bond lengths are in the range 2.109−2.137 Å, and there is small bond alternation. The predicted P−P ring bond orders of 1.29, 1.47, and 1.41 also reveal that bond alternation is less significant. Consequently the P_5 ring retains aromaticity to a large extent.[34]

Second-order perturbational energy analysis in the NBO basis[27] is performed to understand the major interactions conferring stability to the C_s(p) structure. The perturbational analysis examines all possible interactions between filled (donor) NBOs and empty (acceptor) NBOs. The second-order

(32) Nyulaszi, L.; Schleyer, P. v. R. *J. Am. Chem. Soc.* **1999**, *121*, 6872.
(33) (a) Waterman, K. C.; Streitwieser, A.; Blom, R.; Faegri, K., Jr.; Midtgaard, T. *J. Am. Chem. Soc.* **1991**, *113*, 3230. (b) Bohn, R. K.; Haaland, A. *J. Organomet. Chem.* **1966**, *5*, 470. (c) Drouin, B. J.; Cassak, P. A.; Kukolich, S. G. *Inorg. Chem.* **1997**, *36*, 2868. (d) Shibata, S.; Bartell, L. S.; Gavin, R. M. *J. Chem. Phys.* **1964**, *41*, 717. (e) Haaland, A.; Lusztyk, J.; Norak, D. P.; Brunvoll, J. *J. Chem. Soc., Chem. Commun.* **1974**, 54. (f) Ronova, I. A.; Bochvar, D. A.; Chistjakov, A. L.; Struc, Y. T.; Alekseev, J. *J. Organomet. Chem.* **1966**, *5*, 470. (g) Jutzi, P.; Khol, F.; Hofmann, P.; Kruger, C.; Tsay, Y. H. *Chem. Ber.* **1980**, *113*, 757. (h) Alexandratos, S.; Streitwieser, A., Jr.; Schaefer, H. F., III. *J. Am. Chem. Soc.* **1976**, *98*, 7959. (i) Jespersen, K. K.; Chandrashekhar, J.; Schleyer, P. v. R. *J. Org. Chem.* **1980**, *45*, 1608. (j) Waterman, K. C.; Streitwieser, A., Jr. *J. Am. Chem. Soc.* **1984**, *106*, 3138.

stabilization energy associated with delocalization between a donor NBO(i) and acceptor NBO(j) is given as

$$\Delta E_{ij} = q_i \frac{F(i,j)^2}{\epsilon_j - \epsilon_i}$$

where q_i is the donor NBO occupancy, ϵ_i and ϵ_j are NBO energies, and $F(i,j)$ is the off-diagonal NBO Fock matrix element. The perturbational analysis reveals that, among the interactions involving the different donor and acceptor NBOs including all Lewis and non-Lewis orbitals, the strongest stabilization arises from non-Lewis lone-pair orbitals LP_1 on P_1 and LP* on Be. At the B3LYP/6-31G* level, the NBO analysis shows that LP_1 on P_1 exhibits sp-hybrid character and has an occupancy of 1.72 electrons, which is less than that of the idealized Lewis lone pair. LP* on Be has an occupancy of 0.35 electron, and it is the acceptor orbital with 94% contribution from the 2s-orbital and 6% contribution from 2p-orbital. The stabilizing interaction between LP_1 on P_1 and LP* on Be amounts to 123.8 kcal/mol in the C_s(p) structure. It may be noted that the stabilizing interaction between LP_1 on each phosphorus in η^5-(cyclo-P_5) and LP* on Be is ~3.5 kcal/mol in the C_{5v}(s) structure. Though in the C_s(p) structure of the pentaphosphaberyllocene aromatic stabilization of the P_5 ring is lowered as compared to the symmetric sandwich geometries, significant stabilization from the interaction between the lone pair of P_1 and the 2s-orbital of Be (LP*) and the covalent bond formation between the two centers may account for the better stability of the C_s(p) structure over the C_{5v}(e) and C_{5v}(s) geometries. Similar bonding features are also predicted by B3LYP/LANL2DZ, B3LYP/6-311G*//B3LYP/6-31G*, B3LYP/6-31+G*//B3LYP/6-31G*, and B3LYP/6-311+G**//B3LYP/6-31G* calculations.

Investigations on the pentaphosphalithocene anion, starting from the P_5-slipped sandwich geometries, also resulted in the C_s(p) structure. However, in this case the Li−P_1 bond order is significantly lower with a value of 0.12 and the bond is longer. As seen from Figure 3, the P−P bond lengths and bond orders have not changed to any significant extent from that in the sandwich complex. The occupancies on the orbitals LP_1 on P_1 and LP* (2s) on Li are 1.90 and 0.10 electrons, respectively. Due to the longer Li−P_1 separation, the second-order stabilizing interaction between the above two orbitals is 20.5 kcal/mol and is much smaller than the value of 123.8 kcal/mol in $CpBeP_5$. Consequently the C_s(p) structure of the $CpLiP_5$ anion is only about 4 kcal/mol lower than the symmetric sandwich arrangements.

Bending of hydrogens from the plane containing carbons of the Cp ligand is evident in both $[CpLiP_5]^-$ and $CpBeP_5$. The bent angles θ are −0.7° and −4.3° in $[CpLiP_5]^-$ and $CpBeP_5$, respectively, and are more pronounced than in the carbocyclic metallocenes.

It is found that in the symmetric sandwich geometries the distance M−P_5 (center) is longer than that of the M−Cp (center). This is in contrast to the situation in the mixed metallocenes of Fe and Ru[2b,6] that possess shorter values for d_P than d_C. This difference may be attributed to d-orbital participation in the mixed metallocenes of Fe and Ru. In the C_{5v} geometries P−P bond lengths are 2.130 and 2.133 Å respectively in $[CpLiP_5]^-$ and $CpBeP_5$. These lengths are very close to the B3LYP/6-31G* value of 2.127 Å in the free cyclo-P_5 anion. It may be noted that these bond lengths are intermediate between the normal P−P single bond (2.21 Å) and double bond (~2.02 Å) as observed in earlier studies.[2b,4,7−10,21] The P−P distances of 2.134−2.156 Å predicted in the η^5-coordinated cyclo-P_5 ligand in the structures C_s(e) and C_s(s) are in good agreement with the average experimental value[4] of 2.154 Å observed in $[(\eta^5\text{-}P_5)_2Ti]^{2-}$.

The B3LYP/LANL2DZ calculations predict P−P bond lengths of 2.235 Å in the free cyclo-P_5 anion and 2.245−2.258 Å in the sandwich metallocenes. As compared to the B3LYP/6-31G* results the B3LYP/LANL2DZ bond lengths of P−P are uniformly longer (~0.11 Å in free cyclo-P_5 anion and ~0.11−0.12 Å in the metallocenes). The large discrepancy in P−P, M−P, and d_P lengths according to B3LYP/LANL2DZ may be due to the absence of polarization functions in the basis set of phosphorus atoms. In spite of the large discrepancy in the P−P, M−P, and d_P lengths, the B3LYP/LANL2DZ calculations predict bond orders that are very close to those of the B3LYP/6-31G* values. The comparative analysis shows that the bonding characteristics predicted by both B3LYP/6-31G* and B3LYP/LANL2DZ methods are in good agreement.

Structure and Bonding in Decaphospha Analogues of Lithocene Anion and Beryllocene. In the D_{5d} point group, the cyclo-P_5 units have bond lengths of 2.132 and 2.130 Å respectively in the Li and Be complexes. Although these lengths are similar to that in the cyclo-P_5 anion (2.127 Å), only in $[(\eta^5\text{-}P_5)_2Li]^-$ the P−P bond order of 1.396 show a small deviation of about 0.01 from the value of 1.409 in the anionic ligand. In this complex Li−P covalent bonding is hardly significant with bond order less than the threshold value of 0.05. In the case of $(\eta^5\text{-}P_5)_2Be$, there is significant covalent bonding between beryllium and phosphorus atoms as reflected by a Be−P bond order of ~0.14, which is attained at the cost of weakening of P−P bonds (bond order = 1.325). It is observed that the M−P and d_P distances are shorter in the decaphospha analogues than in the pentaphospha analogues. The distance between the two cyclo-P_5 planes in the beryllium complex is 3.726 Å and is comparable to the experimental distance of ~3.6 Å[5] in $[(\eta^5\text{-}P_5)_2Ti]^{2-}$. The separation of 4.510 Å between the cyclo-P_5 planes in $[(\eta^5\text{-}P_5)_2Li]^-$ is longer than the experimental distance of 4.016 Å between the Cp planes in lithocene anion.[16a]

(34) (a) Jug, K. *J. Org. Chem.* 1983, *48*, 1344. (b) Jug, K.; Köster, A. *J. Phys. Org. Chem.* **1991**, *4*, 163. (c) According to the ring current concept given in the above references, the lowest ring bond order is used as an index to define the degree of aromaticity. A cyclic system is nonaromatic when the lowest ring bond order is that of a typical single bond. When it is below that of a single bond, the system is classified as antiaromatic. Aromatic systems are characterized by lowest ring bond order values that are intermediate between normal single and double bonds. As compared to the Wiberg bond orders of CC/PP bonds predicted by B3LYP/6-31G* in the NAO basis, for standard nonaromatic and aromatic systems (ethane, 1.04; Cp anion, 1.41; P_5 anion, 1.41; benzene, 1.44), the C_s(p) structure of $CpBeP_5$ having lowest ring bond order of 1.29 may be classified as moderately aromatic.

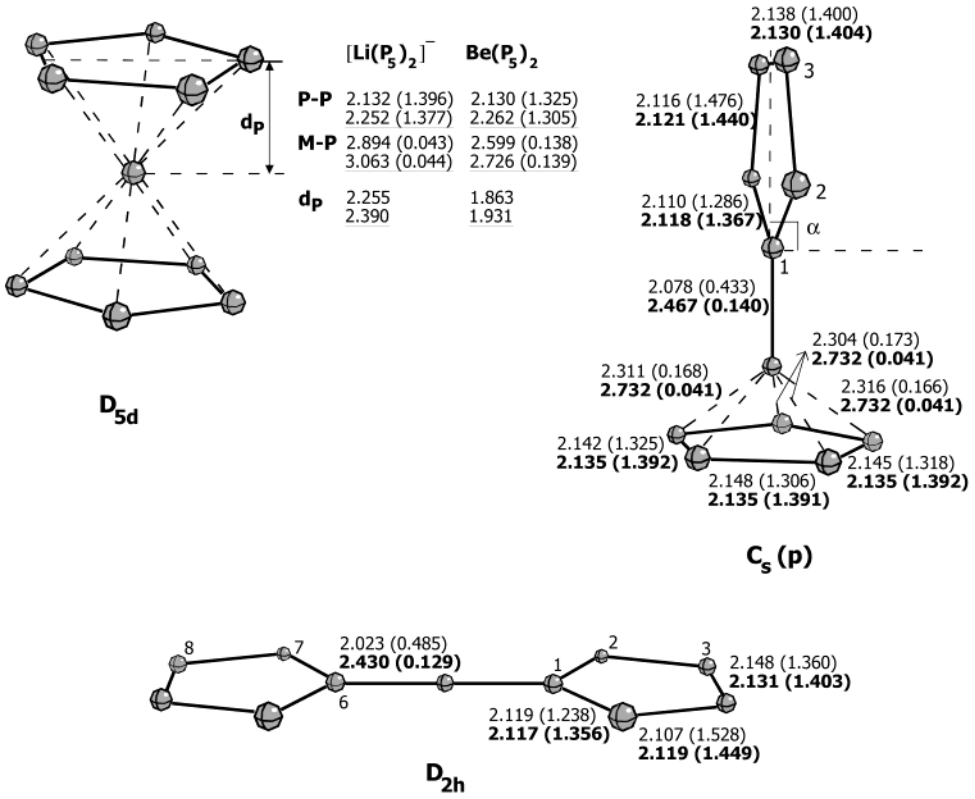

Figure 4. Optimized staggered sandwich D_{5d} and P_5-slipped C_s(p) and D_{2h} geometries of $[(P_5)_2Li]^-$ and $(P_5)_2Be$. The structural parameters of $[(P_5)_2Li]^-$ are shown in bold. Bond lengths are given in angstroms and angles in degrees. Wiberg bond orders are given inside parentheses. The underlined values correspond to B3LYP/LANL2DZ results.

Structural optimization of the slipped sandwich geometries with one η^1-coordinated cyclo-P_5 resulted in the C_s(p) structure (Figure 4). As observed in the pentaphospha analogues, the η^1-coordinated cyclo-P_5 unit is perpendicular to the plane of the η^5-coordinated ligand (cyclo-P_5). The structural and bonding features in the η^1-coordinated cyclo-P_5 unit are very similar to those in the pentaphospha complexes (Figure 3). NBO analysis at B3LYP/6-31G* level reveals an increased occupancy of 0.47 electron on the non-Lewis LP* orbital of Be, which is essentially the 2s-orbital. The second-order stabilization interaction of this orbital with lone-pair LP_1 of P_1 is found to be 122.8 kcal/mol. The η^5-coordinated cyclo-P_5 shows small deviations from the D_{5h} arrangement. The Be−P distances are in the range 2.304−2.316 Å with bond orders ∼0.17 and are about 0.3 Å shorter than in the D_{5d} structure. The Li−P distances of 2.732 Å are ∼0.16 Å shorter than in the staggered geometry, but there is no significant change in the bond orders.

Attempts to optimize the structures in which both cyclo-P_5 units are η^1-coordinated to metal resulted in the D_{2h} structure (Figure 4). The metallocene is planar in the D_{2h} arrangement, and the two P_5 rings are bonded to Be linearly. The covalent Be−P_1 bond length is 2.023 Å and is shorter compared to the value of 2.078 Å in the C_s(p) structure. The bond order of Be−P_1 bond is increased to 0.49 but that of the Li−P_1 bond is reduced in the D_{2h} structure as compared to that in the C_s(p) structure. The calculated bond orders reflect that the P_5 ring has slightly more pronounced bond alternation in the D_{2h} geometry of $(P_5)_2Be$ than in the C_s(p) structure. D_{2h} geometry of the metallocenes is characterized only in the decaphospha analogues $[(P_5)_2Li]^-$ and $(P_5)_2Be$. Such geometries are not found to be potential minima in the biscyclopentadienyl as well as in the mixed metallocenes. Thus the D_{2h} geometry seems to be a unique feature in the decaphosphametallocenes.

Natural Population and Net Charges. The natural population of the valence orbitals and the natural charges on the atomic centers at the optimized lowest energy geometries and the staggered sandwich structures are presented in Tables 3 and 4 respectively for lithium and beryllium complexes. It is striking that the population of the valence orbitals of the metal center increases as the number of P_5 ligands increases. This leads to lowering of the net positive charge on the metal center by the introduction of cyclo-P_5. Thus, in the series $[Cp_2Li]^-$, $[CpLiP_5]^-$, and $[(P_5)_2Li]^-$ lithium has NPA charges of 0.91, 0.86, and 0.77 units at the staggered sandwich geometries. In the carbocyclic system, lithium is nearly unipositive, but in the decaphospha analogue, there is significant population of 0.18 and 0.05 electron in the valence 2s- and 2p-orbitals of Li. If the metal is unipositive, each phosphorus atom of the ligated P_5 rings should possess a net charge of −0.2. The population analysis shows that the net charge on phosphorus atom is less than −0.2 in the penta- as well as decaphospha analogues. In the beryllium complexes Cp_2Be, $CpBeP_5$, and $(P_5)_2Be$, the NPA charge on Be is lowered in the order 1.69, 1.47, and 1.16 units at the staggered sandwich geometries. In $(P_5)_2Be$, population of the 2s- and 2p-orbitals of Be are 0.48 and 0.30 electron. It is obvious that the extent of covalent bond formation between the ligand and the metal center is more

Table 3. Natural Population of Valence Orbitals of Li and the Ligand Atoms and Their Natural Charges at B3LYP/6-31G* Level[a]

			natural population			net charge	
system	point group	element	ns	np	nd	NPA	MPA
$[Cp_2Li]^-$	D_{5d}	Li	0.05	0.05		0.91	0.03
		C	0.96	3.43		−0.40	−0.17
$[CpLiP_5]^-$	C_{5v}(s)	Li	0.09	0.05		0.86	−0.02
		P	1.67	3.49	0.02	−0.19	−0.13
		C	0.97	3.44		−0.41	−0.16
	C_s(p)	Li	0.10	0.05		0.86	0.03
		P_1	1.63	3.68	0.02	−0.33	−0.14
		P_2	1.67	3.44	0.02	−0.13	−0.11
		P_3	1.67	3.47	0.02	−0.17	−0.18
		C	0.97	3.43		−0.41	−0.16
$[(P_5)_2Li]^-$	D_{5d}	Li	0.18	0.04	0.01	0.77	−0.16
		P	1.67	3.49	0.03	−0.18	−0.08
	C_s(p)	Li	0.14	0.04	0.01	0.81	−0.10
		P_1	1.62	3.74	0.02	−0.37	−0.14
		P_2	1.67	3.42	0.02	−0.11	−0.09
		P_3	1.67	3.46	0.02	−0.16	−0.16
		P_6-P_{10}	1.68	3.48	0.03	−0.18	−0.05

[a] Charges predicted by Mulliken population analysis (MPA) are also shown.

Table 4. Natural Population of Valence Orbitals of Be and the Ligand Atoms and Their Natural Charges at the B3LYP/6-31G* Level[a]

			natural population			net charge	
system	point group	element	ns	np	nd	NPA	MPA
Cp_2Be	D_{5d}	Be	0.17	0.13	0.01	1.69	0.53
		C	0.97	3.44		−0.42	−0.18
	C_s(e)	Be	0.24	0.13		1.63	0.36
		C_1	1.08	3.75		−0.84	−0.25
		C_2	0.97	3.31	–	−0.28	−0.17
		C_3	0.97	3.32		−0.29	−0.15
		C_6	1.00	3.43	0.01	−0.43	−0.17
		C_7	1.00	3.44	0.01	−0.43	−0.17
		C_8	1.00	3.43	0.01	−0.43	−0.16
$CpBeP_5$	C_{5v}(s)	Be	0.33	0.20	0.01	1.47	−0.04
		P	1.68	3.42	0.03	−0.13	0.00
		C	1.00	3.44	0.01	−0.43	−0.16
	C_s(p)	Be	0.33	0.16		1.49	0.34
		P_1	1.53	3.91	0.03	−0.46	−0.26
		P_2	1.67	3.35	0.02	−0.05	−0.02
		P_3	1.68	3.38	0.02	−0.09	−0.07
		C_6	1.00	3.42	0.01	−0.42	−0.15
		C_7	1.00	3.43	0.01	−0.43	−0.16
		C_8	1.00	3.43	0.01	−0.43	−0.16
$(P_5)_2Be$	D_{5d}	Be	0.53	0.30	0.01	1.16	−0.58
		P	1.68	3.40	0.03	−0.12	0.06
	C_s(p)	Be	0.48	0.30	0.01	1.21	−0.35
		P_1	1.53	3.94	0.03	−0.50	−0.11
		P_2	1.67	3.33	0.02	−0.04	−0.01
		P_3	1.68	3.37	0.02	−0.08	−0.07
		P_6	1.70	3.36	0.03	−0.09	0.12
		P_7	1.70	3.37	0.03	−0.10	0.12
		P_8	1.70	3.36	0.03	−0.09	0.12

[a] Charges predicted by Mulliken population analysis (MPA) are also shown for comparison.

pronounced in the beryllium complex than in the lithium complex. Another interesting observation in the lowest energy structures is that the unique atom C_1 or P_1 in the ligand having η^1-coordination possesses significant negative charge. Thus for example C_1 in the C_s(e) structure of Cp_2Be exhibits a natural charge of −0.84. This observation indicates that there exists considerable electrostatic attraction between the metal center and C_1 or P_1 in the η^1-mode of bonding of the ligand, besides the covalent bond formation.

From the comparison of orbital interactions in $[(\eta^5\text{-}P_5)_2\text{-}Ti]^{2-}$, it was inferred that cyclo-P_5 behaves as an acceptor while Cp behaves as a donor.[4] In contrast, the present population analysis reveals that Cp has less donor ability than cyclo-P_5. As there are critical differences between the metal−ligand interactions when main group metals are involved (due to absence of valence d-orbitals), we examined the energy levels of the species involved in the present study. Figure 5 compares schematically the valence orbitals of the metal ions and a few highest occupied and lowest vacant molecular orbitals in the anionic ligands and the beryllium complexes. It is seen that the energy gap between the valence orbitals of the metal ion and ligand orbitals is less for the occupied ligand orbitals than the vacant orbitals. Consequently both Cp and cyclo-P_5 can act as donors. As the energy gap is lower for the cyclo-P_5 ligand, it can be a better donor than Cp for the metals under consideration.

Conclusions

The present study shows that the P_5 ligand lowers the relative stability of the complex compared to the Cp ligand. The B3LYP/6-31G* calculations predict heterolytic bond dissociation energies of 737, 690, and 612 kcal/mol respectively for Cp_2Be, $CpBeP_5$, and $(P_5)_2Be$. Single-point calculations using diffuse functions in the basis set at the B3LYP/6-311+G**//B3LYP/6-31G* level yield heterolytic dissociation energies of 702, 667, and 608 kcal/mol for the above systems. Comparison with the experimental value of 635 ± 15 kcal/mol in ferrocene shows that the stability in $CpBeP_5$ and $(P_5)_2$-Be is comparable to that of ferrocene. Lithocene anion and its phospha analogues possess considerably lower stability toward dissociation into ionic fragments.

Staggered sandwich structures of $CpBeP_5$ and $(P_5)_2Be$ are found to be higher order saddle points at the B3LYP/6-31G* level. In these systems the lowest energy structure is one in which the two planar ligands are arranged perpendicular to each other such that one of the ligands, cyclo-P_5, is η^1-coordinated to Be while the second ligand is η^5-coordinated. B3LYP/6-311+G**//B3LYP/6-31G* calculations predict the resulting structure with the C_s point group to be 22 and 28 kcal/mol lower than the staggered sandwich geometry in $CpBeP_5$ and $(P_5)_2Be$, respectively. In the analogous lithocene anions $[CpLiP_5]^-$ and $[(P_5)_2Li]^-$ also the C_s(p) structure is found to be lower than the staggered sandwich geometries by ∼4 kcal/mol though lithocene anion prefers D_{5d} geometry. The C_s(p) structure with the two planar ligands of the metallocence arranged perpendicular to each other is predicted for the first time in metallocenes. This observation is novel as in this lowest energy structure atoms of the η^1-coordinated P_5 ring other than P_1 have negligible interactions with η^5-coordinated ligand and the metal center since the atoms are well separated.

The D_{2h} geometry, in which both of the ligands are η^1-coordinated to the metal center, are characterized only in the decaphospha analogues $[(P_5)_2Li]^-$ and $(P_5)_2Be$. The D_{2h} structure could not be located as potential minima in the biscyclopentadienyl complexes and the pentaphospha ana-

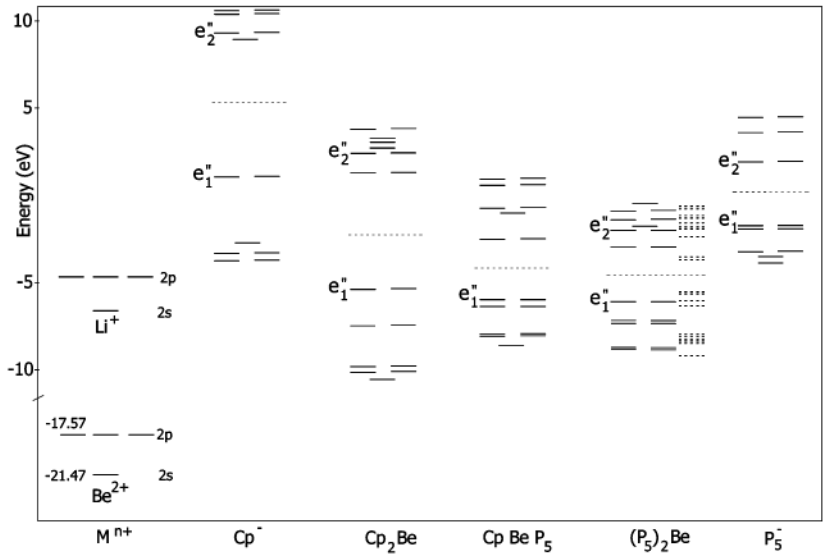

Figure 5. Schematic energy level diagram showing the highest occupied and lowest vacant molecular orbitals of the anionic ligands and beryllocenes of the D_{5h} point group. The broken lines show the energy levels in the C_s(p) geometry of $(P_5)_2$Be.

logues. It is apparent from the present study that the D_{2h} geometry is a unique feature in bis(cyclo-P_5) metallocenes.

Covalent bond formation between beryllium and phosphorus atom P_1 of η^1-(cyclo-P_5) is more pronounced with bond orders of 0.43−0.49 as compared to that between Be and C_1 of η^1-Cp (bond orders ∼0.24−0.27). Bond order analysis reveals that the P_5 ring exhibits moderate aromaticity in the η^1-mode of bonding with Be. In this bonding mode a major stabilizing interaction exists between the lone pair of phosphorus atom P_1 and the 2s-orbital of Be, as revealed by second-order pertubational energy analysis in the natural bond orbital basis. The above aspects favor better stability for the cyclo-P_5-slipped structures than the Cp-slipped structures.

Relative energies and bonding characteristics predicted by B3LYP/LANL2DZ calculations are essentially similar to those of the B3LYP/6-31G* calculations.

Acknowledgment. I thank Professor E. D. Jemmis, University of Hyderabad, India, for interesting discussions and the referees for constructive comments. Optimized geometries of the complexes were generated using MOLDRAW.

Supporting Information Available: Total energies of the complexes and their ionic fragments, Cartesian coordinates of B3LYP/6-31G* optimized geometries, and results on selected NBOs of the lowest energy beryllocenes. This material is available free of charge via the Internet at http://pubs.acs.org.

IC0340027